Earth Sciences

Original article

Miocene paleogeography of northwest Colombia: A review of the sedimentary and magmatic evolution of the Amagá Basin a century after Grosse's work

Paleogeografía del Mioceno en el noroccidente de Colombia: una revisión de la evolución sedimentaria y magmática de la cuenca de Amagá un siglo después del trabajo de Grosse

Sebastián Zapata[1,*], Juan Sebastián Jaramillo-Ríos[2], Gladys Eliana Botello[2], Astrid Siachoque[2], Laura Cristina Calderon-Díaz[2], Agustín Cardona[2], Christy Till[3], Victor Valencia[4]

[1] Group of studies in orogenic systems (GROSSE), Facultad de Ciencias Naturales, Universidad del Rosario, Bogotá, Colombia
[2] Grupo de estudios en geología y geofísica (EGEO), Facultad de Minas, Universidad Nacional de Colombia, Medellín, Colombia
[3] School of Earth and Space Exploration, Arizona State University, Tempe, USA
[4] School of Earth and Environmental Science, Washington State University, Pullman, USA

Abstract

In 1918, the geologist Emile Grosse was commissioned to conduct geological studies in the Amagá Basin, Antioquia, Colombia. In 1923, Grosse finished a comprehensive cartographic work that became the cornerstone for the geology of the northwest (NW) Colombian Andes. Today, 100 years later, the volcanoclastic strata preserved in the Amagá Basin are crucial for understanding major Oligocene to Pliocene tectonic events that occurred in the NW South-American margin, including the fragmentation of the Nazca Plate, the collision of the Panamá-Chocó Block, and the shallowing of the subducted slab. Our contribution includes new mineral chemistry and zircon petrochronological data from the Combia Volcanic Complex and published data to provide a review of the Oligocene to Pliocene deformation, sedimentation, and magmatic patterns in the Amagá Basin and their implications for the tectonic evolution of NW South America. The Amagá Basin was the result of the Eocene to Oligocene uplift of the Western Cordillera followed by the Middle Miocene to Pliocene uplift of both the Central and Western cordilleras, events that modified the Miocene drainage network in the Northern Andes. Coeval with the final Miocene deformation phases in the Amagá basin, the magmatism of the Combia Complex was the result of subduction magmas emplaced in a continental crust affected by strike-slip tectonics.

Keywords: Emile Grosse´s work; Amagá Basin; Combia Volcanic Complex; Mineral chemistry; Northern Andes paleogeography; Zircon petrochronology.

Resumen

En 1918 el geólogo Emile Grosse recibió el encargo de realizar estudios geológicos en la cuenca de Amagá, Colombia. En 1923 Grosse terminó un trabajo cartográfico exhaustivo que se convirtió en la piedra angular para la geología del noroccidente de los Andes colombianos. Hoy, 100 años después, las unidades volcanoclásticas preservadas en la cuenca de Amagá son cruciales para entender los principales eventos tectónicos que ocurrieron en el margen noroccidental suramericano entre el Oligoceno y el Plioceno, incluyendo la fragmentación de la Placa de Nazca, la colisión del Bloque Panamá-Chocó y la subducción plana. El presente trabajo incluye nuevos datos de química mineral y petrocronología en circón del complejo volcánico de Combia e integra datos publicados para proporcionar una revisión de los patrones de deformación, sedimentación y magmatismo del Oligoceno al Plioceno en la cuenca de Amagá y sus implicaciones para la evolución tectónica del

noroccidente suramericano. La cuenca de Amagá fue el resultado del levantamiento del Eoceno al Oligoceno de la cordillera occidental, seguido por el levantamiento del Mioceno Medio al Plioceno de las cordilleras central y occidental. Estas fases de levantamiento modificaron la red de drenaje del Mioceno en los Andes del norte. Coincidiendo con las fases finales de deformación del Mioceno en la cuenca de Amagá, el magmatismo del complejo de Combia fue el resultado de magmas de subducción emplazados en una corteza continental afectada por la tectónica de rumbo.

Palabras clave: Trabajo de Emile Grosse; Cuenca de Amagá; Complejo volcánico del Combia; Química mineral; Paleogeografía de los Andes del norte; Petrocronología en circón.

Introduction

Between 1923 and 1926, the German geologist Emile Grosse completed the geological cartography of the Amagá Basin in northwest Colombia; the study was dedicated to identifying and characterizing the economic resources –particularly coal beds– in the Amagá Basin (**Grosse**, 1926). The results included the identification of two clastic Cenozoic units grouped under the carboniferous tertiary of Antioquia (*Terciario Carbonífero de Antioquia*) (Amagá Formation) and the Combia strata (*Estratos de Combia*) (Combia Volcanic Complex). One hundred years have elapsed since this pivotal work was finished, and several of Grosse´s original observations, such as the distinction between the different sedimentary cycles, the geological relations between the units, and the relative chronology of the sedimentation, magmatism, and deformation events remain valid today.

In the last century, geosciences saw enormous progress, including the development of new techniques (e.g., geochronology, thermochronology, and geochemistry) and the emergence of the plate tectonics theory that led to a greater understanding of Earth systems, which have also been applied to the Amagá Basin. Contributions dealing with various aspects of the tectono-magmatic framework of the basin include studies by **Bissig *et al*.** (2017), **Jaramillo *et al*.** (2019), **Lara *et al*.** (2018), **León *et al*.** (2018), **Montes *et al*.** (2015), **Piedrahita *et al*.** (2017), **Ramírez *et al*.** (2006), **Rodríguez & Zapata** (2014), **Sierra *et al*.** (2012), **Silva-Tamayo *et al*.** (2008, 2020), **Weber *et al*.** (2020), and **Zapata *et al*.** (2020).

The Neogene volcanic and sedimentary strata in the Amagá Basin formed coevally with major Miocene tectonic events that shaped the northwestern segment of the South American Plate, including (i) the break off of the Farallon Plate at ~23 Ma, (ii) the collision of the Panamá-Chocó arc around 12 Ma, and (iii) the slab flattening of the Nazca Plate after ~5 Ma. These events modified the sedimentary routing systems and the connections between the Colombian hinterland and foreland basins (**Jaramillo *et al.***, 2019; **León *et al.***, 2018; **Montes *et al.***, 2019; **Perez-Consuegra *et al.***, 2022; **Silva-Tamayo *et al.***, 2020). In consequence, the Amagá Basin has become a key element to understand the tectonic and paleogeographical evolution of NW South America.

Several studies aim at understanding the correlation between the deformation, magmatic, and sedimentary patterns in the Amagá Basin and the major tectonic events and paleogeographic configuration of the continental margin (**Lara *et al.***, 2018; **Montes *et al.***, 2015; **Piedrahita *et al.***, 2017; **Silva-Tamayo *et al.***, 2020). Despite these efforts, there are still open questions regarding the geometry of the drainage network, the main tectono-structural controls on magmatism, and the relationship between major Miocene tectonic events and deformation patterns.

Here we present new mineral geochemistry and zircon petrochronological data from selected localities in the Combia Volcanic Complex and integrate them with recent regional studies. Our data set includes compositional data of the plagioclase, garnet, and amphibole phases from a pyroclastic rock, and zircon U-Pb geochronology, chemistry, and isotopic (Lu-Hf) data from two andesites and two pyroclastic rocks. These results, combined with published detrital zircon geochronology and geochemical constraints, along with the available thermochronological ages, were used to understand the nature and the tectonic controls of magmatism, and to review and discuss the paleogeographic configuration of the basin.

Geological framework

The Colombian Andes are composed of three parallel and approximately north-south oriented cordilleras separated by two intermountain fluvial valleys: the Cauca Valley between the Western and Central cordilleras and the Magdalena Valley between the Central and Eastern cordilleras (**Figure 1A**). The Amagá and Cauca basins are two approximately north-south lens-shaped hinterland basins along the Cauca Valley (**Figure 1 A, B**) (**Sierra & Marín-Cerón**, 2011). The segmented and lenticular shape of these basins coincides with the narrowest area of the Cauca Valley, around 4.5°N, which has been attributed to a pre-Pleistocene shortening associated with E-W right lateral faults (**Suter** *et al.*, 2008).

In Emile Grosse's original work, the Amagá Basin was delimited between the towns of La Pintada to the south and Santa Fe de Antioquia to the North. However, here we extend the area further south to the town of Chinchiná, where the Colombian Geological Survey has mapped correlatable volcano-sedimentary units (**Figure 1B**). The Amagá Basin sedimentary fill is characterized by Oligocene to Middle Miocene siliciclastic strata, Upper Miocene volcaniclastic layers of the Combia Volcanic Complex and the Irrá-Tres Puertas Formation, and Pliocene conglomeratic successions that include the Santa Fe de Antioquia Formation.

Clastic units of the Amagá Formation

Grosse (1926) defined the carboniferous tertiary of Antioquia as a sedimentary succession composed of conglomerates, sandstones, mudstones, and coal beds unconformably deposited on top of Mesozoic plutonic and metamorphic rocks from the Central Cordillera and the Cretaceous volcaniclastic rocks from the Western Cordillera (**Figure 1C**). Subsequent studies redefined this unit as the Amagá Formation, which included several members based on the abundance of coal beds (e.g. **Sierra** *et al.*, 2003). Recent studies have further divided this unit into Lower and Upper members based on detailed stratigraphy and provenance data interpreting that it was accumulated in braided and meandering depositional systems (for a historical review, see **Silva-Tamayo** *et al.*, 2020).

Detrital zircon fission track data with ages between 41-29 Ma and Oligocene palynomorphs suggest that the Lower Amagá Member was deposited during the late Oligocene (**Lara** *et al.*, 2018; **Montes** *et al.*, 2015; **Piedrahita** *et al.*, 2017; **Zapata** *et al.*, 2020). Maximum depositional ages obtained from detrital zircon U-Pb geochronology suggest that the Upper member was deposited after 21 Ma (**Lara** *et al.*, 2018; **Montes** *et al.*, 2015). Additionally, the older ages associated with the Combia Volcanic Complex suggest that the Upper member was deposited prior to 11 Ma (**Bissig** *et al.*, 2017; **Jaramillo** *et al.*, 2019).

The Santa Fé de Antioquia Formation was proposed by **Lara** *et al.* (2018); it is described as poorly lithified siliciclastic sediments that display facies associations of braided rivers and maximum depositional age at 4.8 Ma. This unit overlays discordantly the Amagá Formation in the northern segment of the basin.

Geology of the volcano-sedimentary formations

Grosse (1926) determined that the Amagá Formation is unconformably overlain by volcanic and clastic strata and is intruded by several volcanic dikes, domes, and hypabyssal porphyries (**Figure 1C**). These volcanic and porphyritic rocks exhibit ages between 11 and 5.2 Ma (**Bernet** *et al.*, 2020; **Bissig** *et al.*, 2017; **Jaramillo** *et al.*, 2019; **Naranjo** *et al.*, 2018; **Leal-Mejia** *et al.,* 2019; **Santacruz** *et al.,* 2021; **Weber** *et al.*, 2020) and are currently grouped into the Combia Volcanic Complex (**Jaramillo** *et al.,* 2019).

The Combia Volcanic Complex has been divided into two members, a volcanic member that includes the intercalation of basalts, andesites, tuffs, and agglomerates, and a sedimentary member consisting mainly of conglomerates, immature sandstones, and siltstones associated with continental debris flows and braided fluvial environments. Porphyritic bodies with tonalitic, granodioritic, and dacitic compositions intrude on both members (**Jaramillo** *et al.*, 2019; **Leal-Mejía** *et al.*, 2019; **Weber** *et al.*, 2020).
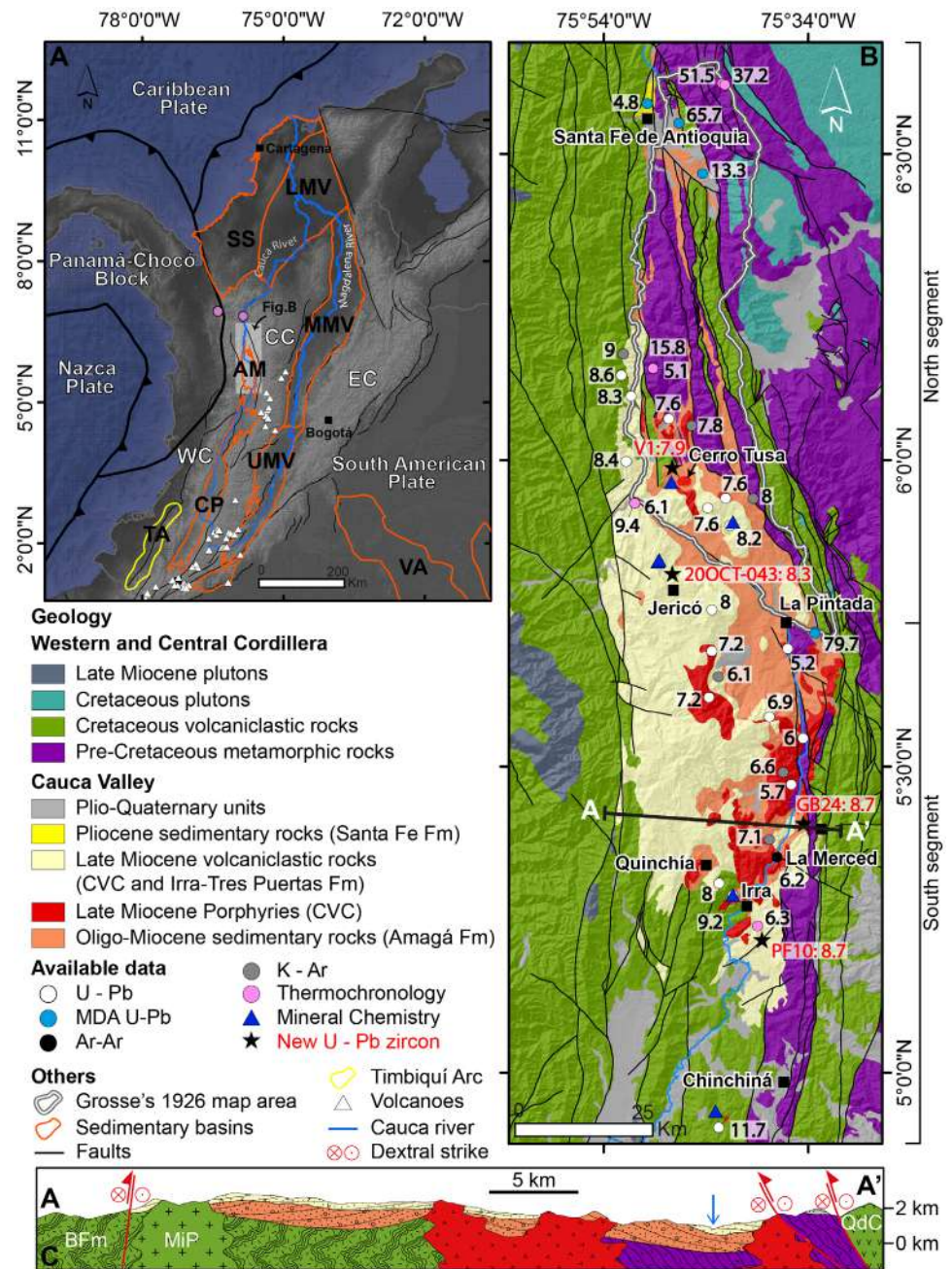
Figure 1. A. Regional map of the Colombian Andes showing the location of the Timbiquí Arc (TA) and Cauca-Patía (CP), Amagá (AM), Sinú-San Jacinto (SS), Lower Magdalena Valley (LMV), Middle Magdalena Valley (MMV), Upper Magdalena Valley (UMV), and Vaúpes-Amazonas (VA) sedimentary basins according to the *Agencia Nacional de Hidrocarburos* (ANH). **B.** Local map of the Amagá Basin showing the ages obtained for the volcanic rocks (**Bernet *et al.*,** 2020; **Bissig *et al.*,** 2017; **Jaramillo *et al.*,** 2019; **Leal-Mejía *et al.*,** 2019; **Santacruz *et al.*,** 2021; **Weber *et al.*,** 2020). Red labels show the new U-Pb zircon ages presented in this work. **C.** Geological profile (A-A') of the south segment of the Amagá Basin showing the discordance relation between CVC and the Amagá Formation and the intrusive relation of the Late Miocene Porphyries (CVC) with the other units. The Cretaceous volcaniclastic rocks were separated in the Barroso Formation (BFm), Mistrató Pluton (MiP), and Quebradagrande Complex (QdC).

Abbreviations: Western Cordillera (WC), Central Cordillera (CC) and Eastern Cordillera (EC), Combia Volcaniclastic Complex (CVC).

The rocks of the Combia Volcanic Complex are characterized by tholeiitic and calc-alkaline compositions, with a typical arc geochemical signature evidenced in a depletion of High-Field Strength Elements, such as Nb, Ta, and Ti. Isotopic Hf, Sr, Nd, and Pb signatures of these rocks suggest variable mantle and crustal inputs (**Bernet et al.**, 2020; **Bissig et al.**, 2017; **Jaramillo et al.**, 2019; **Leal-Mejía et al.**, 2019; **Marín-Cerón et al.**, 2019; **Tassinari et al.**, 2008; **Weber et al.**, 2020). Metaluminous adakite-like and garnet-bearing rocks are also common in between the intrusives of the Combia Volcanic Complex, reflecting variable fractionation trends under heterogeneous crustal architectures (**Bissig et al.**, 2017; **Jaramillo et al.**, 2019; **Weber et al.**, 2020).

The Irrá-Tres Puertas Formation is exposed in the southern segment of the Amagá Basin. This unit comprises conglomerates, sandstones, mudstones, thin layers of coal, tuffaceous sandstones, and pyroclastic rocks deposited by alluvial systems (**Sierra et al.**, 2012). This unit yields a zircon fission track age of 6.3 Ma obtained in a pyroclastic layer (**Toro et al.**, 1999) and is intruded by Upper Miocene porphyries, which means that it is correlatable with the Combia Volcanic Complex.

Cenozoic tectono-magmatic evolution of the Amagá Basin and the bounding cordilleras

The evolution of the Amagá Basin was linked to the exhumation and uplift of the adjacent Western and Central Cordilleras. These orogenic belts consist of crystalline basement rocks formed in contrasting tectonic and paleogeographic settings. The Central Cordillera is mostly composed of Permian to Eocene igneous and metamorphic rocks formed in a continental margin (**Bustamante et al.**, 2016; **Spikings et al.**, 2015; **Villagómez et al.**, 2011) while the predominantly igneous basement of the Western Cordillera corresponds to an oceanic plateau formed to the SW of the continental margin (**Kerr et al.**, 1996). The basement rocks of both cordilleras are intruded by late Cretaceous and Eocene-Paleocene plutonic rocks (**Cardona et al.**, 2018; **Duque-Trujillo et al.**, 2019).

The Central Cordillera basement is the result of several Paleozoic to Cenozoic orogenic cycles, including the accretion of the Caribbean Plateau during the late Cretaceous (**Jaramillo et al.**, 2017; **Spikings et al.**, 2015; **Zapata et al.**, 2020; **Zapata-Villada et al.**, 2021). These orogenic events of erosion and uplift, such as topographic growth during the onset of the Andean orogeny and the collision of the Caribbean Plateau during the Cretaceous, were followed by multiple phases of topographic growth and decay during the Cenozoic (**Restrepo-Moreno et al.**, 2009; **Zapata et al.**, 2021). In contrast, despite being accreted during the late Cretaceous, the onset of uplift and exhumation in the Western Cordillera occurred between the Eocene and the late Oligocene (**Lara et al.**, 2018; **León et al.**, 2018). During the Miocene (~25 to 15 Ma), a Cretaceous to Eocene oceanic arc (Panamá-Chocó Block) collided with the continental margin. As a result of the collision, both the Panamá-Chocó Block and the Western Cordillera experienced phases of uplift and exhumation (**León et al.,** 2018; **Montes et al.**, 2015).

The evolution of the Amagá Basin was shaped by several tectonic events, with most authors agreeing that basin filling and inversion were influenced by strike-slip tectonics (**Lara et al.**, 2018; **Piedrahita et al.**, 2017; **Silva-Tamayo et al.**, 2020). Between the late Oligocene and the Early Miocene, the changes in plate convergence vectors and the fragmentation of the Farallon Plate led to the development of topography in the Western Cordillera and the onset of hinterland sedimentation (**Lara et al.**, 2018; **Silva-Tamayo et al.**, 2020). The oblique collision and docking of the Panamá-Chocó Block between 25 and 12 Ma further promoted uplift and exhumation along the Western Cordillera, provided new sedimentary sources in the basin, and changed the fluvial systems from meandered to braided (**Lara et al.**, 2018; **León et al.,** 2018; **Montes et al.**, 2015). After the collision, between ~11 Ma and ~5 Ma, the Amagá Basin hosted the volcanic and intrusive magmatism of the Combia Volcanic Complex (**Bernet et al.**, 2020; **Bissig et al.,** 2017; **Jaramillo et al.**, 2019; **Weber et al.**, 2020). Finally, the slab flattening of the Nazca Plate after ~5 Ma has been linked to the Late Miocene uplift of the Central Cordillera, the cessation of magmatism, and the deformation of Miocene-Pliocene rocks (**Jaramillo et al.**, 2019; **Pérez-Consuegra et al.**, 2022; **Wagner et al.**, 2017).

Methods

Mineral chemistry and thermobarometry

The mineral compositions of amphibole, plagioclase, and garnet crystals obtained for this study were done in a polished thin (30 μm) section of a pyroclastic rock (Sample CQM-28B; 8.2 ± 0.1 Ma; **Jaramillo et al.**, 2019) at the Department of Lunar and Planetary Sciences of the University of Arizona. After petrographic observations, we selected almost 20 crystals from the mentioned mineral phases for the electron probe micro-analyzer (EPMA). These analyses were performed using CAMECA SX-50 equipment, including quantitative spot analysis done by wavelength-dispersive spectrometry (WDS). The analyses were done with a beam current of 20.0 nA, an accelerating voltage of 15 kV, and a total counting time of 20s. The standards used for element calibrations included "albite-Cr" for Na, "ol-fo92" for Mg and Si, "anor-hk" for Al and Ca, "kspar-OR1" for K, "rutile1" for Ti, "fayalite" for Fe, "rhod-791" for Mn, "chrom-s" for Cr, and "Sp5" for Ni.

Structural formulas of amphibole crystals were calculated following the latest International Mineralogical Association (IMA, 2012) recommendations, which considered that O+OH+F+Cl was equal to 24 atoms per formula unit (apfu). For thermobarometry calculations, amphibole Fe^{3+}/Fe^{2+} ratios were determined assuming 13 cations exclusive of Ca, Na, and K (13-CNK). Cation proportions and formulas for plagioclase and garnet were calculated based on 8 and 12 oxygens, respectively. The summary of the EPMA data and references for normalization and structural mineral formulas are presented in **table 1S,** https://www.raccefyn.co/index.php/raccefyn/article/view/1871/3389.

Amphibole physicochemical parameters, such as crystallization temperatures (T°C), oxygen fugacity (fO_2), and water contents (H_2O_{melt}), were calculated using the equations of **Ridolfi** (2021) while crystallization pressure estimations (MPa) were obtained using the T(°C)-independent calibrations of **Mutch et al.** (2016). Using these procedures, we recalculated published mineral compositions for the same mineral phases in six garnet-bearing porphyries and one andesite from the Combia Volcanic Complex (data from **Bissig et al.,** 2017; **Weber et al.**, 2020).

U-Pb geochronology

Zircons from four samples (V1: Andesite, 20OCT-043: garnet-bearing andesite; PF10 and GB24: pyroclastic rocks) (**Table 1**) were separated at Zirchron LLC®, Tucson, AZ. Zircon U-Pb ages were measured at the Radiogenic Isotope and Geochronology Lab (RIGL) at Washington State University using an Analyte G2 193 excimer laser ablation system coupled with a Thermo-Finnigan™ Element 2 single-collector, inductively coupled, plasma mass spectrometer. The laser parameters included a spot size of 35 μm, a repetition rate of 10 Hz, and an energy of ~5.5 J/cm^2. The procedures followed those of **Chang et al.** (2006), except for the use of the 193 nm laser system instead of the 213 nm laser. The Plešovice standard (337 Ma) was used to calibrate the $^{206}Pb/^{238}U$ and $^{207}Pb/^{235}U$ ages, and the common Pb correction was performed using the ^{207}Pb method. Plots were generated using Isoplot 4.15. The zircon U-Pb data are reported in **table 2S,** https://www.raccefyn.co/index.php/raccefyn/article/view/1871/3390.

We reported the $^{207}Pb/^{206}Pb$ zircon age for grains older than 1000 Ma, while the $^{206}Pb/^{238}U$ age was reported for younger grains. Normal and inverse discordance values were calculated for ages older than 500 Ma, eliminating those that exceeded 20%. The data with more than a 10% error were discarded.

Lu-Hf isotopes in zircon

After the U-Pb analysis, the Lu-Hf isotopic compositions of each sample were analyzed using an Analyte G2 193 nm excimer laser ablation system coupled with a Thermo-Finnigan™ Neptune multi-collector mass spectrometer. Operating parameters included a laser fluence of ~5.5 J/cm^2 and a repetition rate of 10 Hz, following the method discussed by **Fisher et al.** (2014), except that U-Pb dates were not simultaneously determined. The

Table 1. Sample information and average of mineral chemistry of amphibole and petrochronologic data from zircon and amphibole for volcanic rocks of the Combia Volcanic Complex system

Samples	Lat.	Long.	Volcanic facies	U-Pb Age (Ma)	εHf(t)	Ti-in-Zr (°C)	Crystallization parameters			
							P (±50MPa)	T (±22°C)	Log fo_2 (±0.3)	H_2O wt.% (±14%)
V1	5.97	-75.77	Garnet-free andesite porphyry	7.9 ± 0.1	10.8 ± 1.5	698	-	-	-	-
20-OCT-043	5.81	-75.79	Garnet-bearing andesite porphyry	8.3 ± 0.1	7.5 ± 1.3	688	-	-	-	-
PF-10	5.22	-75.64	Pyroclastic rock	8.7 ± 0.1	12.6 ± 1.2	685	-	-	-	-
GB-24	5.41	-75.57	Pyroclastic rock	8.7 ± 0.1	9.7 ± 4.4	692	-	-	-	-
CQM-28B**	5.90	-75.69	Garnet-bearing pyroclastic rock	8.2 ± 0.1	6.7 ± 2.1	-	649	832-907	-12.5	9.0
MJG-132***	5.83	-75.81	Garnet-bearing porphyry	8.9 ± 0.3	-	-	544	873	-11.9	7.2
MJG-134***	5.84	-75.81	Garnet-bearing porphyry	8.6 ± 0.1	-	-	619	888	-11.2	7.9
MW-1***	5.97	-75.77	Garnet-free andesite porphyry	7.9 ± 0.1	-	-	-	-	-	-
CB-P-TB-36*	-	-	Garnet-bearing porphyry	-	-	-	760	885	-10.5	9.3
CB-P-TB-37*	4.92	-75.70	Garnet-bearing porphyry	11.75 ± 0.04	-	764	756	883	-10.8	9.3
CB-P-TB-38*	4.92	-75.70	Garnet-bearing porphyry	-	-	-	719	918	-10.7	8.8
CB-M-AG-25*	5.29	-75.69	Garnet-bearing porphyry	9.25 ± 0.02	-	733	-	-	-	-

References: ***Bissig *et al.,*** 2017; ****Jaramillo *et al.,*** 2017; *****Weber *et al.,*** 2020

output from the ablation cell was mixed with N_2 gas and delivered directly to the Neptune MC-ICPMS. The Plešovice zircon standard ($^{176}Hf/^{177}Hf$ = 0.282482 ± 13) was regularly analyzed between sample blocks to correct the measured $^{176}Hf/^{177}Hf$ of unknowns and reduce inter-laboratory bias. Correction for the isobaric interference of ^{176}Yb and ^{176}Lu on ^{176}Hf was assessed using quality control zircons (**Fisher *et al.***, 2014). Internal 2-sigma precision was ~1.1 εHf. Analyses with less than 25 ratios or internal 2-sigma uncertainty over 2 εHf units were discarded. Present-day εHf values were calculated using the CHUR parameters reported by **Bouvier *et al.*** (2008). Zircon Lu-Hf isotopic data are reported in **table 3S,** https://www.raccefyn.co/index.php/raccefyn/article/view/1871/3391.

Trace element and Lu-Hf isotopes analysis in zircon

Samples with U-Pb and Lu-Hf data were also selected for the trace element analysis including rare earth element (REE) using LA-ICP-MS performed at the Washington State University. Between 8 and 14 zircons were analyzed for each sample. The analysis consisted of two cleaning pulses, 10s washout, 18s gas blank, 40s ablation, and 15s wait before moving the stage. Standards NIST610 and NIST612 and zircon reference 91500 were verified every 15 analyses. Data correction and reduction were performed using the Iolite software. Trace elements and REE zircon data are presented in **table 4S,** https://www.raccefyn.co/index.php/raccefyn/article/view/1871/3391.

Results

New integrated zircon U-Pb, Hf isotopes, trace element results, and mineral chemistry were obtained on several magmatic samples from the Combia Volcanic Complex and the Irrá-Tres Puertas Formation at the northern and southern segments of the Amagá Basin. Here we present some interpretations derived from these results to avoid repetitions in the discussion.

Mineral chemistry and crystallization conditions

Previous studies have documented the existence of andesites, porphyries, and pyroclastic rocks with garnet in the Combia Volcanic Complex (**Bissig *et al.***, 2017; **Jaramillo *et al.***, 2019; **Ramírez *et al.***, 2006; **Weber *et al.***, 2020). Here we present new mineral chemistry from a garnet-bearing pyroclastic rock found in the northeastern segment of the Amagá

Basin, which, together with published data from the other garnet-bearing igneous rocks, can be used to understand deep crustal magmatic processes and the evolution of crustal architecture in the Amagá Basin.

The analyzed pyroclastic rock (Sample CQM-28B) is characterized by a mixture of primary vitric-crystalline and fragmental textures with euhedral to subhedral plagioclase, amphibole, garnet, and quartz phenocrysts, and rounded to angular juvenile-accessory basaltic/andesitic fragments (twinned plagioclase, amphibole, and oxy-hornblende). Additionally, minor rounded accidental lithics (fine-grained sandstones) are embedded into the glassy matrix. Devitrification and jaw-sag textures were also identified.

Mineral chemical results from amphiboles in the Combia Volcanic Complex, including our newly analyzed sample and those from porphyritic rocks presented by **Bissig *et al.*** (2017) and **Weber *et al.,*** (2020), indicate predominantly calcic compositions [0.78 ≤ BCa/B(Ca+Na) ≤ 0.95], classifying as ferri-tschermakite with minor variations to ferri-sadanagaite (**Figure 2A**). The amphibole compositions from porphyritic rocks showed AlT and Ti values of up to 2.75 and 0.24 (in apfu), higher than those in the pyroclastic rock of up to 2.43 and 0.21, respectively (**Table 1S,** https://www.raccefyn.co/index.php/raccefyn/ article/view/1871/3389). These values positively correlate with the Mg number [Mg# =Mg/(Mg+FeT) wt.% oxides], which is between 0.40 and 0.70 in porphyries and between 0.47 and 0.65 in the pyroclastic facies. In contrast, the Fe^{3+}/Fe^{2+} ratios were significantly higher in the pyroclastic rock (0.47 to 2.81) compared to those from the porphyries (0.42 to 1.55; **Table 1S,** https://www.raccefyn.co/index.php/raccefyn/article/view/1871/3389).

Calculated intensive parameters (P, T, fO_2, H_2O_{melt}) using the chemistry of amphiboles for the Combia Volcanic Complex are presented in **table 1**. Despite having similar compositions (**Figure 2A**), the porphyritic rocks exposed in the south present the highest crystallization pressures and temperatures of 526-866 (± 50) MPa and 841-968 (± 22)°C (**Figure 2B**), which can be related to the crystallization of an H_2O-rich (~9.2 wt. %) magma in the middle crust at a depth of ~28 km under elevated magmatic oxidation state (fO_2 = NNO+0 to NNO+3) (**Figure 2C**). Porphyries from the north have overlapping temperatures varying from ~849 to 908 (± 22)°C (**Figure 2B**) but lower pressure emplacement values between 499 to 653 (± 50) MPa (**Figure 2B**), indicating magma fractionation at lower crustal levels at ~ 24 km depth, and moderate magmatic oxidizing conditions (fO_2 = NNO+0 to NNO+1) (**Figure 2C**) with ~7.5 wt. % H_2O in the melt. Amphibole fragments randomly distributed in the vitric-crystalline texture from the pyroclastic rock exhibited similar pressure conditions at ~24 km of depth (**Figure 2B**) but showed the lowest crystallization temperatures among the Combia volcanic facies, between 832 to 870 (± 22 °C), indicating magma fractionation under relatively lower oxidation conditions (fO_2 = NNO-1 to NNO+0) (**Figure 2C**).

Core-to-rim chemical data from plagioclase phenocrysts in the northern porphyries showed variable compositions from bytownite to labradorite (An_{70-90}-Ab_{10-30}-Or_{1-8}) while the southern porphyries and the pyroclastic rock were characterized by plagioclases with labradorite to andesine (An_{30-60}-Ab_{40-70}-Or_{1-5}) (**Table 1S,** https://www.raccefyn.co/index. php/raccefyn/article/view/1871/3389). These compositions suggest that plagioclase phenocrysts from the Combia Volcanic Complex were crystallized at temperatures close to the solidus between 700° to 750°C according to the Ab–An–Or diagram (**Figure 2D**).

Chemical compositions of garnets contain significant amounts of almandine (43-62%), similar grossular and pyrope (11-25% and 11-20%, respectively), and low spessartine (2-19%) (**Figure 2E**). These compositions show two distinct garnet types: (i) one group of Ca- and Mn-rich garnets from the southern porphyries and (ii) garnets with relatively minor Ca- and Mn contents from the northern volcanic rocks which plotted in the high-pressure magmatic crystallization conditions field (HP garnets) of the CaO vs. Mn diagram shown in **figure 2F** (**Harangi *et al.***, 2001). The early crystallization of the almandine-rich garnets indicates that this phase corresponds to the near-liquidus mineral among the distinct Combia volcanic facies suggesting an earlier deeper magmatic fractionation of nearly 40 km (e.g. **Harangi *et al.,*** 2001; **Yuan *et al.,*** 2009).
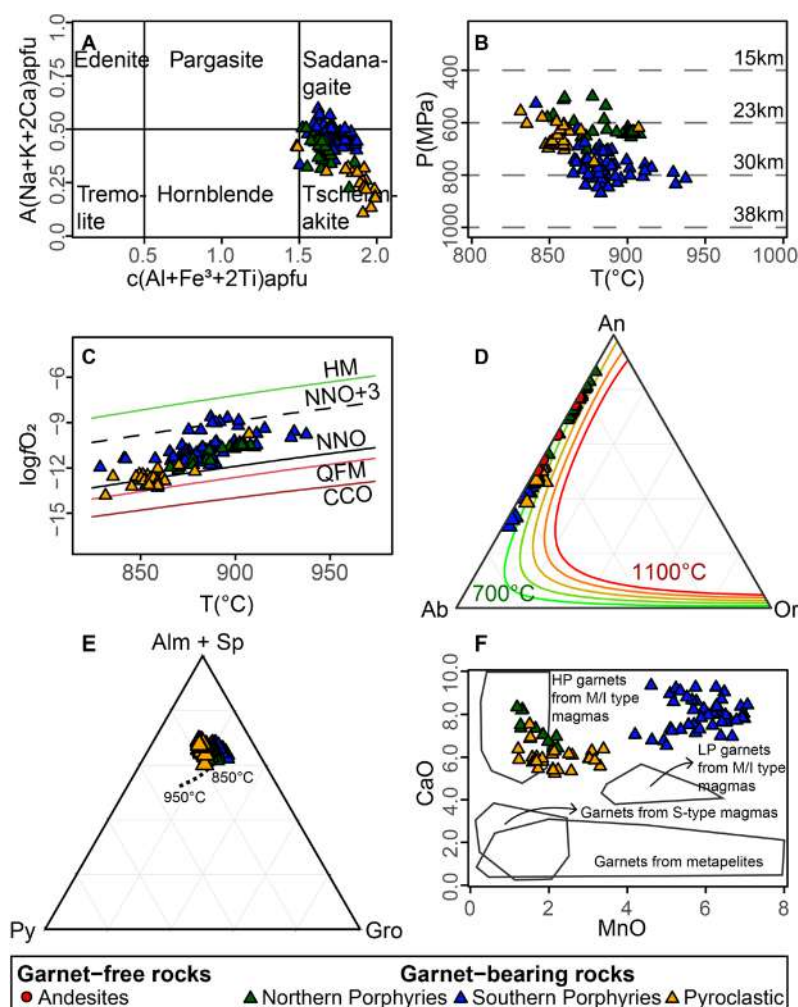
Figure 2. Compositional classification for amphibole, plagioclase, and garnet minerals from porphyries, andesite, and pyroclastic rocks exposed in the Amagá Basin. **A.** Amphibole classification diagram. **B.** Thermobarometry results using the chemistry of amphiboles. **C.** Log fO_2 vs. temperature fields from **Ridolfi** (2021) showing the contrasting amphibole crystallization conditions in the Combia volcanic rocks. **D.** An-Ab-Or ternary diagram of feldspars showing the temperature model from **Elkins & Grove** (1990). **E**. Ternary garnet diagram, the dashed line corresponds to the isobaric cooling between 950 and 850°C (**Alonso-Pérez et al.**, 2009). **F.** Binary MnO vs. CaO plot showing the distinct tectonic setting of garnet formation proposed by **Harangi et al.**, (2001).

Geochronology

U-Pb zircon results were obtained from two lavas and one pyroclastic rock from the Combia Volcanic Complex and one pyroclastic rock from the Irrá-Tres Puertas Formation (**Figure 1B**; **Table 2S,** https://www.raccefyn.co/index.php/raccefyn/article/view/1871/3390).

Samples showed zircons younger than ~9 Ma having Th/U ratios between 0.09 and 1.1 (**Table 2S,** https://www.raccefyn.co/index.php/raccefyn/article/view/1871/3390), suggesting an igneous instead of a metamorphic origin. Older zircon grains with ages between 35 and 2731 Ma and Th/U between 0.12 and 1.1 were interpreted as inherited (**Table 2S,** https://www.raccefyn.co/index.php/raccefyn/article/view/1871/3390). Zircons have subhedral to euhedral shapes, with grain sizes ranging from 50 to 400 μm and length: width (l:w) ratios between 1:1 and 4:1. Cathodoluminescence images showed oscillatory zoning and dark patterns in the magmatic zircons and sector zoning and complex core rims pattern in the inherited ones (**Text 1S**).

Andesite (Sample V1) collected in the Cerro Tusa dome (**Figure 1B**) has a crystallization age of 7.9 ± 0.1 Ma (2σ, n=41) (**Figure 3A, B**) and two zircons with inherited ages of 262 and 1428 Ma. Farther south, a garnet-bearing andesite collected close to the town of Jericó (Sample 20OCT-043) yielded a crystallization age of 8.3 ± 0.1 Ma (2σ, n=15) (**Figure 3C, D**). Lastly, the sample GB24 corresponding to an agglomerate collected close to the town
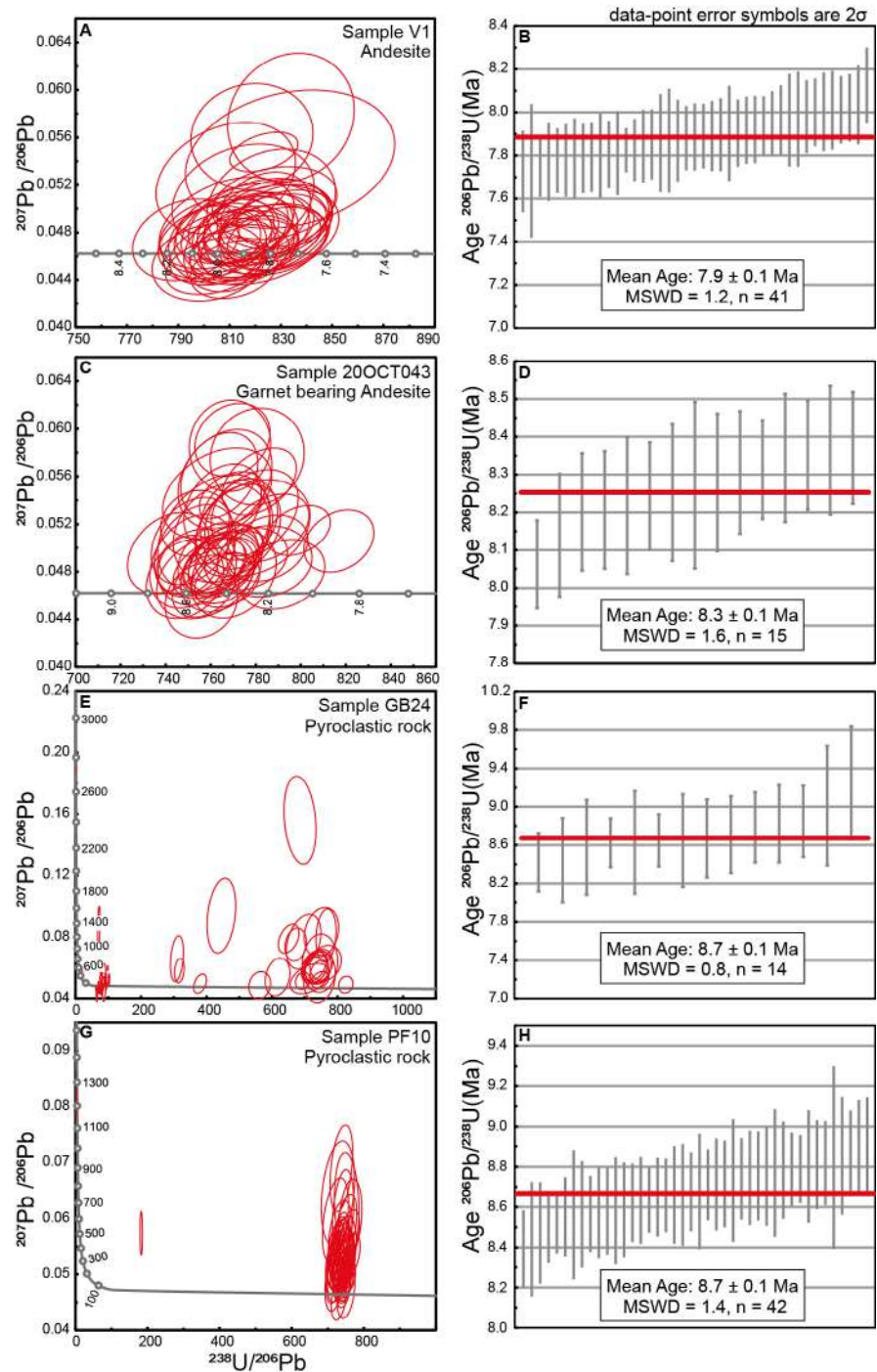

Figure 3. U-Pb geochronological results from the volcanic samples for Combia Volcanic Complex (**A - F**) and Irrá-Tres Puertas Formation (**G-H**). Tera-Wasserburg and weighted average age plots. PDC: Pyroclastic density currents.

of La Merced (Caldas) shows a maximum depositional age of 8.7 ± 0.1 Ma (2σ, n=16) (**xure 3E, F**), which is considered a maximum age for the pyroclastic event. Other zircon crystals have Early Miocene (19 Ma) and Late Cretaceous (69 - 100 Ma) ages and single grains with ages between 309 and 2731 Ma.

The pyroclastic rock sample PF10 was collected in the Irrá-Tres Puertas Formation close to the town of Irrá and yielded an age of 8.7 ± 0.1 Ma (2σ, n=42), which can be related to the maximum age for the pyroclastic accumulation. Also, two zircons were 35 and 1195 Ma.

Zircon chemistry and Hf isotopes

Trace elements and Hf isotopes in zircons were conducted in the same samples used for geochronology. Additionally, we reviewed the trace element data from porphyritic rocks in the southern segment of the Amagá Basin presented by **Bissig *et al.*** (2017).

The magmatic facies of the Combia Volcanic Complex have similar trace elements in zircon compositions, with few differences in some specific elements that we discuss next. Zircons show a positive slope between the light rare earth elements (LREE) and the heavy rare earth elements (HREE). However, the garnet-bearing andesite (20OCT-043) was characterized by a lower slope when compared with all the other samples (**Figure 4A**). All samples showed a flat to weakly negative Eu trend with Eu/Eu* ratios between 0.20 and 0.91, except for the garnet-free andesite that exhibited a stronger negative anomaly (Eu/Eu* between 0.03 and 0.08) (**Figure 4B**). Furthermore, all samples have a positive Ce anomaly, which is more pronounced in the porphyries and the pyroclastic rocks compared to the andesites. Ti values had low variations, between 4.9 and 6.5 ppm, in the pyroclastic and andesitic samples corresponding to temperatures between 683.0 and 704.3 °C while in porphyries these values were more scattered, between 4.1 and 19.8 ppm, corresponding to temperatures from 668.1 to 804.6 °C (**Figure 4B**).

Th/U ratios exhibited a correlation with the presence of magmatic garnet. The U content of the samples ranged between 100 and 1000 ppm, while the Th values ranged between 10 and 700 ppm. The garnet-free magmatic facies had higher Th/U values, between 0.19 and 1.07, while the garnet-bearing had relatively lower values ranging from 0.04 to 0.33 (**Figure 4C, D**).

Yb/Gd showed a trend between the garnet-free volcanic rocks, whereas porphyries and garnet-bearing andesite show a data cloud (**Figure 4D**). The pyroclastic rocks and andesites had higher Yb/Gd ratios ranging from 15 to 80, followed by the porphyritic rocks with ratios between 10 and 50. Finally, garnet-bearing andesites had lower values ranging from 5 to 14. Additionally, all samples plot in an array of magmatic arc zircons in the Nb/Yb vs U/Yb diagram (**Figure 4E**). εHf$_{(t)}$ values in the garnet-bearing rocks varied between 4.7 and 9.12, while garnet-free rocks exhibited a wider εHf$_{(t)}$ range with values between -0.9 and 13.8 (**Figure 4F**).

Discussion

After Grosse's fundamental cartographic work on the Amagá Basin, significant progress has been made in understanding specific aspects associated with the history of this basin, including its structural style and geometry, the evolution of its sedimentary systems, and its tectono-magmatic evolution (**Bernet *et al.***, 2020; **Bissig *et al.*,** 2017; **Jaramillo *et al.,*** 2019; **Lara *et al.*,** 2018; **Piedrahita *et al.*,** 2017; **Silva-Tamayo *et al.*,** 2020). Moreover, the sedimentary and volcaniclastic filling of this basin has provided relevant data on major issues concerning the Cenozoic tectonic evolution of northwestern South America, such as the collision of the Panamá-Chocó Block and the subduction history of the Nazca Plate (**Jaramillo *et al.,*** 2019; **Lara *et al.*,** 2018; **Montes *et al.*,** 2015; **Silva-Tamayo *et al.*,** 2020).

Based on the data presented in this study, on a review of recent provenance, and the thermochronological constraints from various regions in the northern Colombian Andes, including the Central and Western cordilleras and the Amagá, Upper and Middle
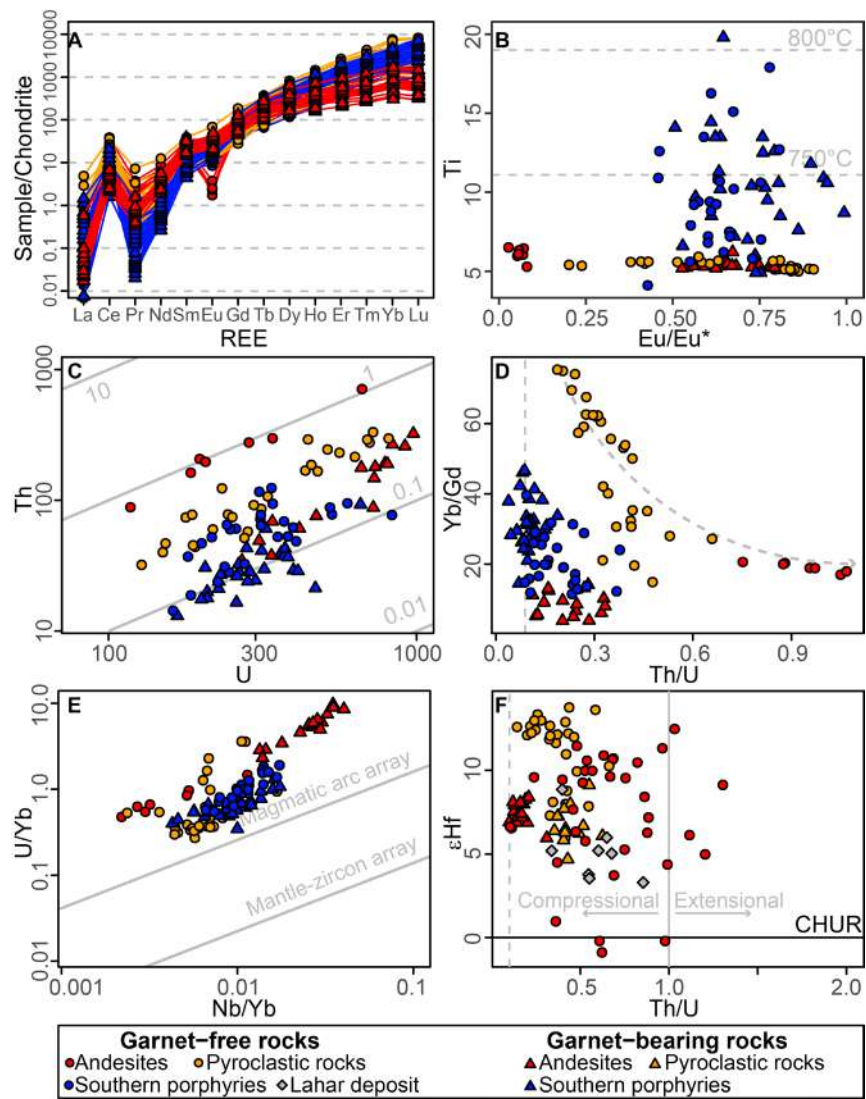
Figure 4. A. Spider plot of REE normalized to chondrite (**McDonough & Sun**, 1995). **B.** Eu/Eu* calculated as $Eu_N/(Sm_N*Gd_N)^{0.5}$ vs. Ti (ppm) and the inferred saturation temperatures (**Ferry & Watson**, 2007)., **C.** Th v. U and Th/U ratios, **D.** Th/U vs Yb/Gd. **E.** Nb/Yb vs. U/Yb, annotations are from **Grimes** *et al.*, (2015). **F.** Th/U vs $\varepsilon Hf_{(t)}$, annotations are from **McKay** *et al.*, (2018). Zircon chemical and isotopic data from garnet-free and garnet-bearing porphyries are from **Bissig** *et al.*, (2017), $\varepsilon Hf_{(t)}$ data from garnet-bearing pyroclastic rocks and some other andesites are from **Jaramillo** *et al.* (2019). The dashed vertical lines in **figure 4 D** and **F** correspond to Th/U=0.01.

Magdalena, and Caribbean basins, we investigated the paleogeographic and structural development of the Amagá Basin with special emphasis on the significant role of strike-slip tectonics on its Cenozoic evolution (**Montes** *et al.,* 2019; **Silva-Tamayo** *et al.*, 2020).

Basin configuration and paleogeography

In Grosse's study, the Amagá Basin was found to have two main filling phases separated by an angular unconformity: the Oligocene to Middle Miocene Amagá Formation, characterized by sedimentation without magmatic activity, and the Middle Miocene to Pliocene Combia Volcanic Complex, which recorded a period of intra-arc magmatism in the basin. The stratigraphic analysis of the Amagá Formation suggests that it was deposited in fluvial systems within several intermountain pull-apart basins (**Lara** *et al.*, 2018;

Silva-Tamayo *et al.*, 2020). For the Combia Volcanic Complex, the magmatic activity was contemporaneous with sedimentation in fluvial environments and the denudation of volcanic edifices (**Sierra *et al.***, 2003; **Ramírez *et al.***, 2006).

Available detrital zircon ages from the Amagá Formation (Lower and Upper members) include 1273 zircon ages from 11 samples distributed in three localities along the basin (**Bissig *et al.***, 2017; **Jaramillo *et al.***, 2019; **Lara *et al.***, 2018; **Montes *et al.***, 2015; **Naranjo *et al.***, 2018; **Santacruz *et al.***, 2021; **Zapata *et al.***, 2020). The broad stratigraphic and spatial distribution of this detrital database can be used to reconstruct the regional configuration of the Amagá Basin and its fluvial connection with or isolation from other basins.

The Oligocene to Early Miocene Lower Amagá Formation is more compositionally mature than the Middle Miocene Upper Amagá Formation (**Lara *et al.***, 2018). The Lower Amaga Formation is characterized by dominant late Cretaceous to early Eocene (100 - 45 Ma) zircon age populations that account for 86% of the ages, with a minor component of early Cretaceous (1.7%) and Permo-Triassic (12%) age populations whereas the Upper Member exhibits similar late Cretaceous to early Eocene (67%) and Permo-Triassic (24%) populations besides the presence of a diagnostic late Eocene to Oligocene (3.2%) Panamanian population (**Table 2**) (**Figure 5**).

Late Cretaceous to early Eocene zircon ages are characteristic of primary and reworked volcaniclastic and plutonic rocks in the axis and western flank of the Central Cordillera and in the axis and eastern flank of the Western Cordillera (**Bustamante *et al.***, 2016; **Duque-Trujillo *et al.***, 2019; **Pardo-Trujillo *et al.***, 2020; **Villagómez *et al.***, 2011; **Zapata-Villada *et al.***, 2021). The high proportion of late Cretaceous detrital zircons suggests that most of their sources were related to the erosion of the magmatic arcs and volcaniclastic sequences exposed in both cordilleras (**Cardona *et al.,*** 2020; **Duque-Trujillo *et al.***, 2019; **Jaramillo *et al.***, 2017; **Pardo-Trujillo *et al.,*** 2020; **Zapata-Villada *et al.***, 2021). Such affinity to the bounding cordilleras confirms the intra-mountainous character of this basin. The younger Eocene to Oligocene sources in the Upper Amagá Formation have been considered a major tracer of the 25-12 Ma docking of the Panamá-Chocó Block, which is exposed in the western flank of the Western Cordillera (**Lara *et al.,*** 2018; **Silva-Tamayo *et al.***, 2020).

In the Upper Amagá Member, there is a higher abundance of lithic fragments, particularly those of plutonic and metamorphic origin, compared to the Lower Amagá Member. The latter is distinguished by a low percentage of volcanic lithics (**Lara *et al.***, 2018). This pattern, coupled with the observed rise in the proportion of Permian and Triassic zircon ages (as depicted in **figure 5**), implies that sources from the Central Cordillera region became more prominent.

The Western Cordillera has been subject to various cooling phases and there is available thermochronological data and thermal history modeling suggesting at least two major phases of cooling from the Eocene to late Oligocene and Middle Miocene to Pliocene (**León *et al.***, 2018; **Villagómez *et al.***, 2011). In contrast, the Central Cordillera

Table 2. Summary of the geochronological results with the age ranges in percentage

Lithostratigraphic Unit	N (grain number)	Ages (%)					
		0 - 10 Ma	10 - 30 Ma	30 - 45 Ma	45 - 100 Ma	100 - 130 Ma	>130 Ma
Lower Amagá Fm	706	0.0	0.0	0.0	86.1	1.7	12.2
Upper Amagá Fm	567	0.0	3.7	3.2	67.5	0.9	24.7
Combia Volcanic Complex (Pyroclastic rocks)	180	62.8	10.0	0.6	12.1	1.2	13.3
Combia Volcanic Complex (Crystalline rocks)	252	73.4	2.0	0.8	4.4	3.2	16.3
Santa Fe de Antioquia Fm	113	9.7	0.0	0.0	30.1	0.0	60.2

has a more extensive thermochronological dataset, which has been interpreted as a result of different phases of exhumation and deformation between the late Cretaceous and the Miocene (**Duque-Palacio et al.**, 2021; **Pérez-Consuegra et al.,** 2022; **Restrepo-Moreno et al.**, 2009; **Zapata et al.**, 2020).

An integrated regional thermo-kinematic modeling of the available data on the Central Cordillera revealed rapid exhumation and uplift during the late Cretaceous followed by topographic decay during the Paleogene and uplift during the Miocene (**Zapata et al.**, 2021). This scenario where the Central Cordillera was an old and denuded landscape that was re-activated in the Miocene is consistent with the previously mentioned increase in detrital sources from the Central Cordillera during the Middle Miocene (**Zapata et al.**, 2021).
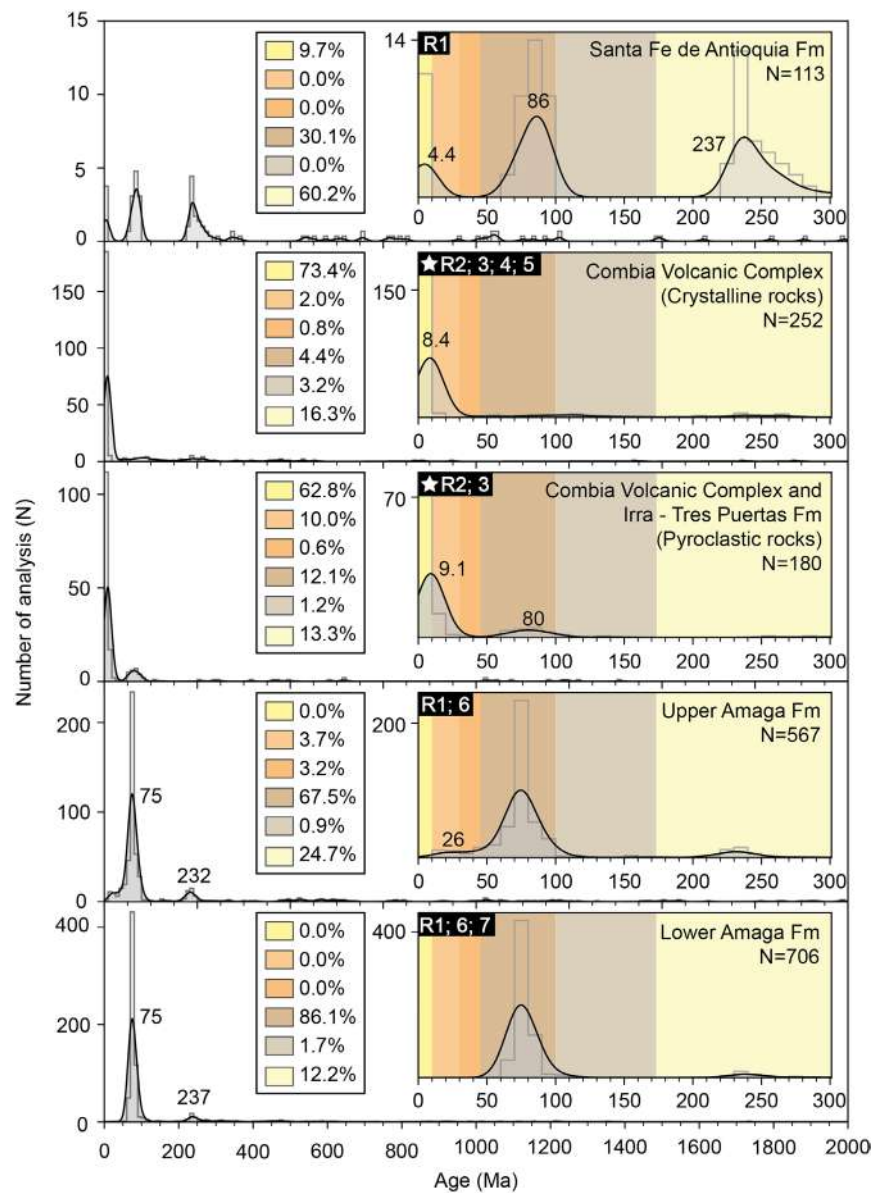

Figure 5. Kernel density estimates of zircon U-Pb ages data compiled from Cenozoic units in the Amagá Basin. Black squares contain the references of the compiled data while white stars denote the data presented in this contribution (R1: **Lara et al.**, 2018; R2: **Bissing et al.**, 2017; R3: **Jaramillo et al.**, 2019; R4: **Naranjo et al.**, 2018; R5: **Santacruz et al.**, 2021; R6: **Montes et al.**, 2015; R7: **Zapata et al.**, 2020).

In summary, provenance signatures and modeled thermochronological data indicate Eocene to Oligocene exhumation and uplift in the Western Cordillera, while the Central Cordillera was a decaying positive relief. Furthermore, both cordilleras underwent exhumation and uplift during the Middle Miocene to Pliocene, a final phase that was more intense in the Western Cordillera. The observations further suggest that deformation and exhumation were more prolonged and intense to the west, within the suture zone of the Western Cordillera, which documents the oblique approach of the Panamá Arc to northwestern South America (**Lara *et al.***, 2018; **León *et al.***, 2018; **Montes *et al.***, 2019).

Additional insights on the geometrical and structural evolution of the Amagá Basin can be evaluated from its relationship with other Oligo-Miocene basins. **Montes *et al.*** (2015) proposed a fluvial connection between the Amagá, the Caribbean Sinú-San Jacinto, and the Lower Magdalena basins based on the synchronous apparition of Eocene (30 to 45 Ma) zircons from the Panamá-Chocó Block in these basins. Similarly, the presence of Eocene to Miocene zircons in the Upper Magdalena Basin served to propose a fluvial connection between the Amagá, the Cauca-Patía, the Upper Magdalena, and the Amazon basins (**Montes *et al.***, 2021). Based on a regional interpretation of the sedimentary facies in the Sinú-San Jacinto and Lower Magdalena basins, **Mora *et al.*** (2018) proposed a model that suggests a long-lived connection between these basins (Proto-Cauca).

The presence of the Eocene to Oligocene zircon ages indicates that the Panamá-Chocó Block became the source area of the Amagá and San Jacinto basins; however, it does not necessarily imply a fluvial connection between these basins. Additionally, the presence of an Eocene volcanic arc in the southern part of the Western Cordillera (Timbiquí Arc) presents a valid source for the Eocene zircon grains in the Upper Magdalena Valley and other basins in the south; in consequence (**Zapata *et al.***, 2023), a fluvial connection between the Panamá-Chocó Block and the Amazonia is not required.

Based on geomorphometric data, **Pérez-Consuegra *et al.*** (2022) proposed that the connection between the Amagá and the San Jacinto basins occurred only after 7 Ma. This interpretation aligns with the existence of a relatively high Western Cordillera and a low Central Cordillera, which may have facilitated west-to-east drainage connections between the Amagá and Middle Magdalena basins. Hence, we favor the paleogeographic model that proposes a connection between the Amagá Basin and the eastern Middle Magdalena Basin presented in **Zapata *et al.*** (2023).

However, it should be noted that the configuration of the paleo-drainage network in the Amagá Basin remains an open research topic and that regional provenance and stratigraphic correlation are necessary to resolve and clarify this discussion. The available data still leaves room for further investigation and refinement of the paleogeographic configuration, the subsidence mechanisms, and the topographic evolution of the Amagá Basin.

The Combia Volcanic Complex: Late Miocene structurally controlled volcanic arc

The new U-Pb zircon results from volcanic rocks of the Combia Volcanic Complex exhibit ages between 8.7 and 7.9 Ma, which together with published geochronological data (**Bissig *et al.***, 2017; **Jaramillo *et al.***, 2019, **Santacruz *et al.***, 2021; **Weber *et al.***, 2020) suggest that the volcanic record of the Combia Volcanic Complex in the Amagá Basin only lasted ~6 Ma, with older ages in the south (11.8 - 4.7 Ma) and apparently younger in the north (9.0 - 5.2 Ma).

Previous geochemical and isotopic studies conducted on the Combia Volcanic Complex have recognized geochemical groups exhibiting tholeiitic, calc-alkaline, and adakite-like signatures (**Bernet *et al.***, 2020; **Bissig *et al.***, 2017; **Borrero & Toro-Toro**, 2016; **Jaramillo *et al.***, 2019; **Weber *et al.***, 2020), as well as exotic garnet-bearing igneous rocks (**Bissig *et al.***, 2017; **Weber *et al.***, 2020; this contribution). These compositional heterogeneities are widely distributed along the Amagá Basin and are evident in the Hf results (including those reported here), which range from -0.9 to 13.8, as well as in the variations of oxygen fugacity observed in the amphiboles (**Figures 2C** and **4F**).

Extensive discussions have been conducted on the relation between HREE and LREE elements and La/Yb or Sr/Y ratios as tracers of MOHO depth and crustal thickness (e.g., **Luffi & Ducea**, 2022 and references therein). These inferences are based on the fact that intermediate to silicic magmas that evolved from mantle magmas are fractionated at the base of the crust. These tracers were evaluated for rocks of the Combia Complex by **Jaramillo et al.** (2019) and suggested highly variable crustal depths between 14 and 51 km. Consistent with mineral chemistry and the absence of an Eu anomaly in the zircon REE trends (**Figures 2** and **4 A, B**), they also indicate that fractionation or emplacement occurred at intermediate to shallow crustal depths between 17-50 km (**Bissig et al.**, 2017; **Borrero & Toro-Toro**, 2016; **Jaramillo et al.**, 2019; **Weber et al.**, 2020). These findings suggest the evolution of mantle-derived magmas that underwent different degrees of crustal assimilation and fractionation at various depths within the crust (**Borrero & Toro-Toro**, 2016; **Jaramillo et al.**, 2019; **Weber et al.**, 2020).

These variations in crustal thickness are also reflected in the occurrence of garnet-bearing facies, which, together with adakite-like magmatism and mixtures of radiogenic and contaminated isotopic signatures, are indicative of a thicker continental crust. Furthermore, the preservation of primary magmatic garnet phases in volcanic rocks is often associated with fast and structurally controlled magmatic migration between deep and upper crustal levels (**Harangi et al.**, 2001). The high water content and calc-alkaline nature of mafic magmas suggest that they were generated by flux melting of the mantle in the presence of water in a subduction zone. Therefore, it is possible to relate the magmatic suites of the Combia Volcanic Complex to a thick continental crust that was locally extended by strike-slip tectonics and cut by deep-seated faults, which facilitated the emplacement of subduction-related juvenile magmas.

The Combia Complex was likely related to the formation subduction magmas that were emplaced during strike-slip extensional tectonics associated with the long-term evolution of the Amagá Basin in a regional pull-apart configuration (**Jaramillo et al.**, 2019; **Sierra et al.**, 2012). This tectonic scenario was already proposed by **Jaramillo et al.** (2019) and **Weber et al.** (2020).

Pliocene sedimentation inversion of the Amagá Basin and termination of vulcanism in the Combia Volcanic Complex

Most authors agree on the existence of a final Late Miocene to Pliocene exhumation phase in the Central Cordillera; the time of this event was well constrained by **Pérez-Congruegra et al.** (2022) using fully reset AHe ages of ~7 Ma below the apatite partial retention zone. Moreover, geogenomic studies have shown that high-elevation palms colonized the northern segment of the Central Cordillera during the Pliocene (**Sanín et al.**, 2022). This deformation phase coincided with the deposition of the conglomeratic Santa Fe de Antioquia Formation after 4.8 Ma, which is characterized by a major Permo-Triassic population (60.2%), followed by a late Cretaceous to Eocene peak (30.1%) and a Miocene population (9.7%), with minor Precambrian peaks; this detrital signature shows higher affinity with the Central Cordillera than the Amagá Formation (**Figure 5**). These independent pieces of evidence suggest significant surface uplift in the Northern segment of the Central Cordillera between 7 and 3 Ma.

The available geochronological database shows that magmatism in the Amagá Basin was totally terminated at ~5.0 Ma (**Bissig et al.**, 2017; **Jaramillo et al.**, 2019; **Naranjo et al.**, 2018; **Santacruz et al.**, 2021), which together with the installation of the Pleistocene to a recent volcanic arc in the south of the Central Cordillera has been interpreted as the result of slab shallowing after 5 Ma at least north of the 5.5 °N (**Wagner et al.**, 2017 and references therein).

Conclusions

1. The provenance data compiled and presented in this contribution suggest that the Amagá Basin resulted from Oligocene to Pliocene sediment accumulation in an intermountain pull-apart basin between the Western and Central Cordilleras. The basin

history is directly related to the uplift phases of the bounding cordilleras. During the Oligocene, uplift in the Western Cordillera created space for intermountain sediment accumulation, while the Central Cordillera remained as a low and decaying positive relief. Subsequently, during the docking of the Panamá-Chocó Block, both cordilleras experienced further phases of uplift after 20 million years. However, the Western Cordillera underwent more intense exhumation, deformation, and uplift. During the Pliocene, both cordilleras experienced deformation, uplift, and exhumation.

2. The obtained crystallization parameters for the calc-alkaline andesite porphyries and pyroclastic facies of the Combia Volcanic System demonstrate that the porphyritic rocks found in the southernmost portion of the Amagá Basin were produced from a hydrous magma that experienced higher oxidizing (fo_2) conditions in comparison to the coeval porphyries and pyroclastic rocks found in the northern region of the basin. These rocks were formed under moderate to lower magmatic oxidation conditions. The presence of magmas that were derived and fractionated under contrasting crustal architectures with varying degrees of crustal assimilation are interpreted as the products of a short-lived volcanic arc controlled by upper plate strike-slip tectonics

3. We highlight the Amagá Basin as an example of a strike-slip basin in a subduction orogen characterized by structurally controlled heterogeneous and discontinuous magmatism and multiple phases of uplift of the bounding tectonic blocks and a likely complex short-lived connection with the adjacent basins.

Supplementary material

See table 1S in https://www.raccefyn.co/index.php/raccefyn/article/view/1871/3389

See table 2S in https://www.raccefyn.co/index.php/raccefyn/article/view/1871/3390

See table 3S in https://www.raccefyn.co/index.php/raccefyn/article/view/1871/3391

See table 4S in https://www.raccefyn.co/index.php/raccefyn/article/view/1871/3392

Acknowledgments

Conflicts of interest

The authors declare that they have no conflicts of interest that may in any way influence the transparency or objectivity of the peer review and publication process or financial conflicts resulting from employer-employee relationships, patents, fees, advisory, or research funding by companies.

Author contributions

SZ: Interpretation of the data, manuscript writing; JSJ: Data collection and interpretation, manuscript writing; GEB.: Data collection and interpretation, manuscript writing; AS.: Data interpretation, manuscript writing; LCCD: Data interpretation, manuscript writing; AC: Data collection and interpretation, manuscript writing; CT: Data collection, manuscript writing; VV: Data collection and analysis

References

Alonso-Pérez, R., Müntener, O., Ulmer, P. (2009). Igneous garnet and amphibole fractionation in the roots of island arcs: Experimental constraints on andesitic liquids. *Contributions to Mineralogy and Petrology*, *157*(4), 541-558. https://doi.org/10.1007/s00410-008-0351-8

Bernet, M., Mesa-García, J., Chauvel, C., Ramírez-Londoño, M. J., Marín-Cerón, M. I. (2020). Thermochronological, petrographic and geochemical characteristics of the Combia Formation, Amagá basin, Colombia. *Journal of South American Earth Sciences*, *104* (September), 1-21. https://doi.org/10.1016/j.jsames.2020.102897

Bissig, T., Leal-Mejía, H., Stevens, R. B., Hart, C. J. R. (2017). High Sr/Y magma petrogenesis and the link to porphyry mineralization as revealed by garnet-bearing I-type granodiorite porphyries of the middle Cauca Au-Cu belt, Colombia. *Economic Geology*, *112*(3), 551-568. https://doi.org/10.2113/econgeo.112.3.551

Borrero, C., Toro-Toro, L. M. (2016). Vulcanismo de afinidad adaquítica en el miembro inferior de la formación Combia (mioceno tardío) al sur de la subcuenca de Amaga, Noroccidente de Colombia. *Boletin de Geologia*, *38*(1), 87-100. https://doi.org/10.18273/revbol.v38n1-2016005

Bouvier, A., Vervoort, J. D., Patchett, P. J. (2008). The Lu-Hf and Sm-Nd isotopic composition of CHUR: Constraints from unequilibrated chondrites and implications for the bulk composition of terrestrial planets. *Earth and Planetary Science Letters*, *273*(1-2), 48-57. https://doi.org/10.1016/j.epsl.2008.06.010

Bustamante, C., Archanjo, C. J., Cardona, A., Vervoort, J. D. (2016). Late Jurassic to Early Cretaceous plutonism in the Colombian Andes: A record of long-term arc maturity. *Bulletin of the Geological Society of America*, *128*(11-12), 1762-1779. https://doi.org/10.1130/B31307.1

Cardona, A., León, S., Jaramillo, J. S., Montes, C., Valencia, V., Vanegas, J., Bustamante, C., Echeverri, S. (2018). The Paleogene arcs of the northern Andes of Colombia and Panama: Insights on plate kinematic implications from new and existing geochemical, geochronological and isotopic data. *Tectonophysics*, *749*(October), 88-103. https://doi.org/10.1016/j.tecto.2018.10.032

Cardona, A., León, S., Jaramillo, J. S., Schmitt, A. K., Mejía, D., Arenas, J. C. (2020). Cretaceous Record from a Mariana– to an Andean–Type Margin in the Central Cordillera of the Colombian Andes. In Gómez, J. & Pinilla–Pachon, A.O. *The Geology of Colombia* (Vol. 2)*, Servicio Geológico Colombiano.

Chang, Z., Vervoort, J. D., McClelland, W. C., Knaack, C. (2006). U-Pb dating of zircon by LA-ICP-MS. *Geochemistry, Geophysics, Geosystems*, *7*(5), 1-14.

Duque-Palacio, S., Seward, D., Restrepo-Moreno, S. A., García-Ramos, D. (2021). Timing and rates of morpho-tectonic events in a segment of the Central and Western cordilleras of Colombia revealed through low-temperature thermochronology. *Journal of South American Earth Sciences*, *106*, 103085. https://doi.org/https://doi.org/10.1016/j.jsames.2020.103085

Duque-Trujillo, J., Bustamante, C., Solari, L., Gómez-Mafla, Á., Toro-Villegas, G., Hoyos, S. (2019). Reviewing the Antioquia batholith and satellite bodies: A record of Late Cretaceous to Eocene syn-to post-collisional arc magmatism in the central cordillera of Colombia. *Andean Geology*, *46*(1), 82-101. https://doi.org/10.5027/andgeov46n1-3120

Elkins, L. T., Grove, T. L. (1990). Ternary feldspar experiments and thermodynamic models. *American Mineralogist*, *75*(5-6), 544-559.

Ferry, J. M. & Watson, E. B. (2007). New thermodynamic models and revised calibrations for the Ti-in-zircon and Zr-in-rutile thermometers. *Contributions to Mineralogy and Petrology*, *154* (4), 429-437. https://doi.org/10.1007/s00410-007-0201-0

Fisher, C. M., Vervoort, J. D., Dufrane, S. A. (2014). Accurate Hf isotope determinations of complex zircons using the "laser ablation split stream" method. *Geochemistry, Geophysics, Geosystems*, *15*(1), 121-139. https://doi.org/10.1002/2013GC004962

Grimes, C. B., Wooden, J. L., Cheadle, M. J., John, B. E. (2015). "Fingerprinting" tectono-magmatic provenance using trace elements in igneous zircon. *Contributions to Mineralogy and Petrology*, *170*(5-6), 1-26. https://doi.org/10.1007/s00410-015-1199-3

Grosse, E. (1926). El Terciario Carbonífero de Antioquia. In *Das Kohlentertiär Antioquias, Verlag von Dietrich Reimer (Ernst Vohsen)* (p. 361).

Harangi, S, Downes, H., Kósa, L., Szabó, C. S., Thirlwall, M. F., Mason, P. R. D., Mattey, D. (2001). Almandine garnet in calc-alkaline volcanic rocks of the Northern Pannonian Basin (Eastern-Central Europe): Geochemistry, petrogenesis and geodynamic implications. *Journal of Petrology*, *42*(10), 1813-1844. https://doi.org/10.1093/petrology/42.10.1813

Jaramillo, J. S., Cardona, A., León, S., Valencia, V., Vinasco, C. (2017). Geochemistry and geochronology from Cretaceous magmatic and sedimentary rocks at 6°35′ N, western flank of the Central cordillera (Colombian Andes): Magmatic record of arc growth and collision. *Journal of South American Earth Sciences*, *76*, 460-481. https://doi.org/10.1016/j.jsames.2017.04.012

Jaramillo, J. S., Cardona, A., Monsalve, G., Valencia, V., León, S. (2019). Petrogenesis of the late Miocene Combia volcanic complex, northwestern Colombian Andes: Tectonic implication of short term and compositionally heterogeneous arc magmatism. *Lithos*, *330-331*, 194-210. https://doi.org/10.1016/j.lithos.2019.02.017

Kerr, A. C., Tarney, J., Marriner, G. F., Nivia, A., Klaver, G. T. H., Saunders, A. D. (1996). The geochemistry and tectonic setting of late Cretaceous Caribbean and Colombian volcanism. *Journal of South American Earth Sciences*, *9*(1-2 SPEC. ISS.), 111-120. https://doi.org/10.1016/0895-9811(96)00031-4

Lara, M., Salazar-Franco, A. M., Silva-Tamayo, J. C. (2018). Provenance of the Cenozoic siliciclastic intramontane Amagá Formation: Implications for the early Miocene collision between Central and South America. *Sedimentary Geology*, *373*, 147-162. https://doi.org/10.1016/j.sedgeo.2018.06.003

Leal-Mejía, H., Shaw, R. P., Melgarejo i Draper, J. C. (2019). Spatial-temporal migration of granitoid magmatism and the phanerozoic tectono-magmatic evolution of the Colombian Andes. In *Frontiers in Earth Sciences*. https://doi.org/10.1007/978-3-319-76132-9_5

León, S., Cardona, A., Parra, M., Sobel, E. R., Jaramillo, J. S., Glodny, J., Valencia, V. A., Chew, D., Montes, C., Posada, G., Monsalve, G., Pardo-Trujillo, A. (2018). Transition From Collisional to Subduction-Related Regimes: An Example From Neogene Panama-Nazca-South America Interactions. *Tectonics*, *37*(1), 119-139. https://doi.org/10.1002/2017TC004785

Luffi, P., Ducea, M. N. (2022). Chemical Mohometry: Assessing Crustal Thickness of Ancient Orogens Using Geochemical and Isotopic Data. *Reviews of Geophysics*, *60*(2), 1-42. https://doi.org/10.1029/2021RG000753

Marín-Cerón, M. I., Leal-Mejía, H., Bernet, M., Mesa-García, J. (2019). Late Cenozoic to modern-day volcanism in the Northern Andes: A geochronological, petrographical, and geochemical review. In *Frontiers in Earth Sciences* (Issue January). https://doi.org/10.1007/978-3-319-76132-9_8

McDonough, W. F., Sun, S. S. (1995). The composition of the Earth. *Chemical geology*, *120*(3-4), 223-253.

McKay, M. P., Jackson, W. T., Hessler, A. M. (2018). Tectonic stress regime recorded by zircon Th/U. *Gondwana Research*, *57*, 1-9. https://doi.org/10.1016/j.gr.2018.01.004

Leal-Mejía, H., Shaw, R. P., Melgarejo i Draper, J. C. (2019). Spatial-temporal migration of granitoid magmatism and the phanerozoic tectono-magmatic evolution of the Colombian Andes. In Cediel, F., Shaw, R.P. (eds) *Geology and Tectonics of Northwestern South America. Frontiers in Earth Sciences*. Springer, Cham. https://doi.org/10.1007/978-3-319-76132-9_5

Montes, C., Rodríguez-Corcho, A. F., Bayona, G., Hoyos, N., Zapata, S., Cardona, A. (2019). Continental margin response to multiple arc-continent collisions: The northern Andes-Caribbean margin. *Earth-Science Reviews*, *198*(April), 102903. https://doi.org/10.1016/j.earscirev.2019.102903

Montes, C., Silva, C. A., Bayona, G. A., Villamil, R., Stiles, E., Rodríguez-Corcho, A. F., Beltrán-Triviño, A., Lamus, F., Muñoz-Granados, M. D., Pérez-Angel, L. C., Hoyos, N., Gómez, S., Galeano, J. J., Romero, E., Baquero, M., Cardenas-Rozo, A. L., von Quadt, A. (2021). A Middle to Late Miocene Trans-Andean Portal: Geologic Record in the Tatacoa Desert. *Frontiers in Earth Science*, *8*(January), 1-19. https://doi.org/10.3389/feart.2020.587022

Montes, C., Cardona, A., Jaramillo, C., Pardo, A., Silva - Tamayo, J. C., Valencia, V., Ayala, C., Pérez-Angel, L. C., Rodríguez-Parra, L., Ramírez, V., Niño, H. (2015). Middle Miocene closure of the Central American Seaway. *Science*, *348*(6231), 226-229.

Mora, J. A., Oncken, O., Le Breton, E., Mora, A., Veloza, G., Vélez, V., de Freitas, M. (2018). Controls on forearc basin formation and evolution: Insights from Oligocene to Recent tectono-stratigraphy of the Lower Magdalena Valley basin of northwest Colombia. *Marine and Petroleum Geology*, *97*(June), 288-310. https://doi.org/10.1016/j.marpetgeo.2018.06.032

Mutch, E. J. F., Blundy, J. D., Tattitch, B. C., Cooper, F. J., Brooker, R. A. (2016). An experimental study of amphibole stability in low-pressure granitic magmas and a revised Al-in-hornblende geobarometer. *Contributions to Mineralogy and Petrology*, *171*(10), 1-27. https://doi.org/10.1007/s00410-016-1298-9

Naranjo, A., Horner, J., Jahoda, R., Diamond, L. W., Castro, A., Uribe, A., Perez, C., Paz, H., Mejia, C., Weil, J. (2018). La Colosa Au porphyry deposit, Colombia: Mineralization styles, structural controls, and age constraints. *Economic Geology*, *113*(3), 553-578. https://doi.org/10.5382/econgeo.2018.4562

Pardo-Trujillo, A., Cardona, A., Giraldo, A. S., León, S., Vallejo, D. F., Trejos-Tamayo, R., Plata, A., Ceballos, J., Echeverri, S., Barbosa-Espitia, A., Slattery, J., Salazar-Ríos, A., Botello, G. E., Celis, S. A., Osorio-Granada, E., Giraldo-Villegas, C. A. (2020). Sedimentary record of the Cretaceous–Paleocene arc–continent collision in the northwestern Colombian Andes: Insights from stratigraphic and provenance constraints. *Sedimentary Geology*, *401,* 1-24. https://doi.org/10.1016/j.sedgeo.2020.105627

Pérez-Consuegra, N., Hoke, G. D., Fitzgerald, P., Mora, A., Sobel, E. R., Glodny, J. (2022). Late Miocene–Pliocene onset of fluvial incision of the Cauca River Canyon in the Northern Andes. *Bulletin of the Geological Society of America*, *134*(9-10), 2453-2468. https://doi.org/10.1130/B36047.1

Piedrahita, V. A., Bernet, M., Chadima, M., Sierra, G. M., Marín-Cerón, M. I., Toro, G. E. (2017). Detrital zircon fission-track thermochronology and magnetic fabric of the Amagá Formation (Colombia): Intracontinental deformation and exhumation events in the northwestern Andes. *Sedimentary Geology*, *356*, 26-42. https://doi.org/10.1016/j.sedgeo.2017.05.003

Ramírez, D., López, A., Sierra, G., Toro, G. (2006). Edad y proveniencia de las rocas volcánico sedimentarias de la formación Combia en el suroccidente antioqueño - Colombia. *Boletín de Ciencias de La Tierra*, *0*(19), 09-26.

Restrepo-Moreno, S. A., Foster, D. A., Stockli, D. F., Parra-Sánchez, L. N. (2009). Long-term erosion and exhumation of the "Altiplano Antioqueño", Northern Andes (Colombia) from apatite (U-Th)/He thermochronology. *Earth and Planetary Science Letters*, *278* (1-2), 1-12. https://doi.org/10.1016/j.epsl.2008.09.037

Ridolfi, F. (2021). Amp-tb2: An updated model for calcic amphibole thermobarometry. *Minerals*, *11*(3), 1-9. https://doi.org/10.3390/min11030324

Rodríguez, G., Zapata, G. (2014). Denominada andesitas basálticas de El Morito - Correlación regional con eventos magmáticos de arco. *Boletín de Geología*, *36*, 85-102.

Sanín, M. J., Mejía-Franco, F. G., Paris, M., Valencia-Montoya, W. A., Salamin, N., Kessler, M., Olivares, I., Jaramillo, J. S., Cardona, A. (2022). Geogenomics of montane palms points to Miocene–Pliocene Andean segmentation related to strike-slip tectonics. *Journal of Biogeography*, *49*(9), 1711-1725. https://doi.org/10.1111/jbi.14327

Santacruz, L., Redwood, S. D., Cecchi, A., Matteini, M., Botelho, N. F., Ceballos, J., Starling, T., Molano, J. C. (2021). The age and petrogenesis of reduced to weakly oxidized porphyry intrusions at the Marmato gold deposit, Colombia. *Ore Geology Reviews*, *131*(December 2020), 103953. https://doi.org/10.1016/j.oregeorev.2020.103953

Sierra, G. M., Marín-Cerón, M. I., MacDonald, W. D. (2012). Evolución tectónica de la cuenca de tracción Irrá. Evidencias de cambios en el movimiento de rumbo de la zona de falla de Romeral, zona norte de la Cordillera central de los Andes, Colombia. *Boletín de Ciencias de La Tierra*, *32*, 143-159. http://www.redalyc.org/articulo.oa?id=169525406013

Sierra, G. M., Silva-Tamayo, J. C., Correa, L. G. (2003). Estratigrafía secuencias de la Formación Amagá. *Boletín de Ciencias de La Tierra*, *15*, 9-22.

Sierra, G. M., Marín-Cerón, M. I. (2011). Petroleum geology of Colombia: Amagá, Cauca and Patía basins. *Agencia Nacional de Hidrocarburos, 2*, 25-38.

Silva-Tamayo, J. C., Lara, M., Salazar-Franco, A. M. (2020). Oligocene – Miocene Coal–Bearing Successions of the Amagá Formation, Antioquia, Colombia: Sedimentary Environments, Stratigraphy, and Tectonic Implications. *The Geology of Colombia,* Chapter 11, Servicio Geológico Colombiano.

Spikings, R., Cochrane, R., Villagomez, D., Van der Lelij, R., Vallejo, C., Winkler, W., Beate, B. (2015). The geological history of northwestern South America: From Pangaea to the early collision of the Caribbean Large Igneous Province (290-75 Ma). *Gondwana Research*, *27*(1), 95-139. https://doi.org/10.1016/j.gr.2014.06.004

Suter, F., Sartori, M., Neuwerth, R., Gorin, G. (2008). Structural imprints at the front of the Chocó-Panamá indenter: Field data from the North Cauca Valley Basin, Central Colombia. *Tectonophysics*, *460*(1-4), 134-157. https://doi.org/10.1016/j.tecto.2008.07.015

Tassinari, C. C. G., Pinzón, F. D., Buena Ventura, J. (2008). Age and sources of gold mineralization in the Marmato mining district, NW Colombia: A Miocene-Pliocene epizonal gold deposit. *Ore Geology Reviews*, *33*(3-4), 505-518. https://doi.org/10.1016/j.oregeorev.2007.03.002

Vargas, C. A., Mann, P. (2013). Tearing and breaking off of subducted slabs as the result of collision of the Panama arc-indenter with Northwestern South America. *Bulletin of the Seismological Society of America*, *103*(3), 2025-2046. https://doi.org/10.1785/0120120328

Villagómez, D., Spikings, R., Magna, T., Kammer, A., Winkler, W., Beltrán, A. (2011). Geo-chronology, geochemistry and tectonic evolution of the Western and Central cordilleras of Colombia. *Lithos*, *125*(3-4), 875-896. https://doi.org/10.1016/j.lithos.2011.05.003

Wagner, L. S., Jaramillo, J. S., Ramírez-Hoyos, L. F., Monsalve, G., Cardona, A., Becker, T. W. (2017). Transient slab flattening beneath Colombia. *Geophysical Research Letters*, *44*(13), 6616-6623. https://doi.org/10.1002/2017GL073981

Weber, M., Duque, J., Hoyos, S., Cárdenas-Rozo, A., Gómez-Tapias, J., Wilson, R. (2020). The Combia Volcanic Province: Miocene Post-Collisional Magmatism in the Northern Andes. *Geology of Colombia*, *3*(November), 161-172. https://doi.org/10.1201/9780203498743-15

Yuan, C., Sun, M., Xiao, W., Wilde, S., Li, X., Liu, X., Long, X., Xia, X., Ye, K., Li, J. (2009). Garnet-bearing tonalitic porphyry from East Kunlun, Northeast Tibetan Plateau: Implications for adakite and magmas from the MASH Zone. *International Journal of Earth Sciences*, *98* (6), 1489-1510. https://doi.org/10.1007/s00531-008-0335-y

Zapata-Villada, J. P., Cardona, A., Serna, S., Rodríguez, G. (2021). Late Cretaceous to Paleocene magmatic record of the transition between collision and subduction in the Western and Central Cordillera of northern Colombia. *Journal of South American Earth Sciences*, *112* (P1), 103557. https://doi.org/10.1016/j.jsames.2021.103557

Zapata, S., Patiño, A., Cardona, A., Parra, M., Valencia, V., Reiners, P., Oboh-Ikuenobe, F., Genezini, F. (2020). Bedrock and detrital zircon thermochronology to unravel exhumation histories of accreted tectonic blocks: An example from the Western Colombian Andes. *Journal of South American Earth Sciences*, *103*(April), 1-15. https://doi.org/10.1016/j.jsames.2020.102715

Zapata, S., Zapata-Henao, M., Cardona, A., Jaramillo, C., Silvestro, D., Oboh-Ikuenobe, F. (2021). Long-term topographic growth and decay constrained by 3D thermo-kinematic modeling: Tectonic evolution of the Antioquia Altiplano, Northern Andes. *Global and Planetary Change*, *203*(May), 103553. https://doi.org/10.1016/j.gloplacha.2021.103553

Zapata, S., Calderón-Díaz, L., Jaramillo, C., Oboh-Ikuenobe, F., Piedrahita, J. C., Rodríguez-Cuevas, M., Cardona, A., Sobel, E. R., Parra, M., Valencia, V., Patiño, A., Jaramillo-Rios, J. S., Flores, M., Glodny, J. (2023). Drainage and sedimentary response of the Northern Andes and the Pebas system to Miocene strike-slip tectonics: A source to sink study of the Magdalena Basin. *Basin Research, 00*, 1-44. https://doi.org/10.1111/bre.12769